Evidence for Pygmy and Giant Dipole Resonances in ^{130}Sn and ^{132}Sn

P. Adrich,[1,4] A. Klimkiewicz,[1,4] M. Fallot,[1] K. Boretzky,[1] T. Aumann,[1] D. Cortina-Gil,[5] U. Datta Pramanik,[1] Th. W. Elze,[2] H. Emling,[1] H. Geissel,[1] M. Hellström,[1] K. L. Jones,[1] J. V. Kratz,[3] R. Kulessa,[4] Y. Leifels,[1] C. Nociforo,[3] R. Palit,[2] H. Simon,[1] G. Surówka,[4] K. Sümmerer,[1] and W. Waluś[4]

(LAND-FRS Collaboration)

[1]*Gesellschaft für Schwerionenforschung (GSI), D-64291 Darmstadt, Germany*
[2]*Institut für Kernphysik, Johann Wolfgang Goethe-Universität, D-60486 Frankfurt am Main, Germany*
[3]*Institut für Kernchemie, Johannes Gutenberg-Universität, D-55099 Mainz, Germany*
[4]*Instytut Fizyki, Uniwersytet Jagielloński, PL-30-059 Kraków, Poland*
[5]*Universidad de Santiago de Compostela, 15706, Santiago de Compostela, Spain*
(Received 29 April 2005; published 21 September 2005)

The dipole strength distribution above the one-neutron separation energy was measured in the unstable ^{130}Sn and the double-magic ^{132}Sn isotopes. The results were deduced from Coulomb dissociation of secondary Sn beams with energies around 500 MeV/nucleon, produced by in-flight fission of a primary ^{238}U beam. In addition to the giant dipole resonance, a resonancelike structure (''pygmy resonance'') is observed at a lower excitation energy around 10 MeV exhausting a few percent of the isovector $E1$ energy-weighted sum rule. The results are discussed in the context of a predicted new dipole mode of excess neutrons oscillating out of phase with the core nucleons.

DOI: 10.1103/PhysRevLett.95.132501 PACS numbers: 24.30.Cz, 25.60.−t, 25.70.De, 27.60.+j

Studies of the multipole response of atomic nuclei have been a rich source of information on the variety of nuclear excitation modes as well as on the nature of the underlying nuclear interactions (see, e.g., Ref. [1]). With the advent of the first-generation exotic-beam facilities, it was natural to raise the question of the multipole response of unstable nuclei. Restricting the discussion to dipole excitations of neutron-rich, medium-heavy, and heavy nuclei, it is expected to find a stronger fragmentation of strength than in stable nuclei, with significant components located in an energy domain well below that of the giant dipole resonance (GDR).

The nature of the low-lying excitations is a matter of ongoing discussion. A concept that attracts most of the attention is a picture of the excess neutrons at the nuclear surface (neutron skin) oscillating against the core of the nucleus—a mode commonly referred to as a ''soft'' or ''pygmy'' dipole resonance (PDR). This interpretation was already discussed in the early 1990s [2,3] and is strongly supported by recent relativistic RPA calculations [4–6]. Low-lying $E1$ strength in unstable neutron-rich nuclei is currently also discussed in the context of the astrophysical r-process nucleosynthesis [7].

In contrast to the theoretical achievements, not much experimental data on multipole strength distributions in unstable nuclei exist at present. In one of the previous experiments of our collaboration, the $E1$ strength above the neutron-emission threshold up to 30 MeV excitation energy was probed in oxygen isotopes, including nuclei close to the drip line such as ^{20,22}O [8]. A considerable fraction of strength was detected at energies below the GDR domain. On theoretical grounds, however, it was concluded to be rather due to single-particle transitions than to a collective soft mode. The $E1$ strength below the neutron-separation threshold in ^{20}O was measured by another group using the complementary technique of virtual photon scattering at intermediate energies [9]. Dipole strength considerably exceeding a shell model prediction was reported.

For heavier nuclei, the $E1$ strength was measured up to date only in stable nuclei with small or medium neutron excess. Very recently, in a real-photon scattering experiment, a resonancelike concentration of $E1$ strength has been observed below the neutron-separation threshold in semimagic $N = 82$ stable isotones of mass $A \approx 140$ [10] and around the neutron threshold in ^{208}Pb [11].

In this Letter, we report on measurements of the dipole strength in the unstable nuclei ^{130,132}Sn, performed with the LAND-FRS facility at GSI, Darmstadt. As an experimental tool the electromagnetic (''Coulomb'') excitation of a secondary high-energy beam in a high-Z target was exploited. In this process, $E1$ transitions are excited with very high cross sections while integrated cross sections due to other multipole excitations are typically on the 10% level. The dipole strength distribution and the photo-neutron cross sections, from the neutron-separation threshold up to 25 MeV excitation energy, could be deduced from the measured electromagnetic dissociation cross sections by means of the semiclassical method of virtual photons [12,13].

The beam of ^{132}Sn and about 20 other isotopes of similar mass-to-charge (A/Z) ratio were produced by in-flight fission of a ^{238}U primary beam with an intensity of 1.4×10^8 ions/s incident on a Be target. Isotopes were

selected according to their magnetic rigidity by the fragment separator FRS [14]. The secondary beams were delivered to the experimental setup with energies around 500 MeV/nucleon. For ^{132}Sn, the intensity amounted to about 10 ions/s on the target. The incoming projectiles were unambiguously identified event by event by determining their magnetic rigidity (with a position measurement in the dispersive midfocal plane of the FRS), time of flight, and energy loss. Projectiles were excited in a secondary ^{208}Pb target (468 mg/cm^2). Additional measurements were performed with a ^{12}C target (370 mg/cm^2) and without target. The results presented in this Letter were deduced from the data effectively collected for 4 days of beam time. The experimental setup and a beam-identification plot are shown in Fig. 1.

The momenta of the neutron(s) emerging after projectile dissociation were measured with the large area neutron detector (LAND) [15] situated about 11 m downstream from the target. At 500 MeV neutron energy, the intrinsic efficiency of LAND for single neutron detection reaches 0.9. In the case of a two-neutron event, the efficiency of reconstructing both neutrons is about 50% and drops further for higher multiplicities. The time of flight is measured with a resolution of $\sigma_t = 300$ ps, the position with $\sigma_{x,y,z} = 4.4$ cm.

Gamma rays following neutron emission were detected with the 4π Crystal Ball spectrometer surrounding the target. The high granularity of the array, consisting of 160 NaI crystals, allows correction of the Doppler shift, which results in a γ-ray full-energy-peak resolution of around 15%. The measurement of the total energy carried away by γ radiation suffered from a background due to radiation of atomic origin occurring during the passage of the projectile through the target material. To reduce the uncertainty of the γ-energy measurement, only the forward hemisphere of the array was used in the off-line analysis. In this way,

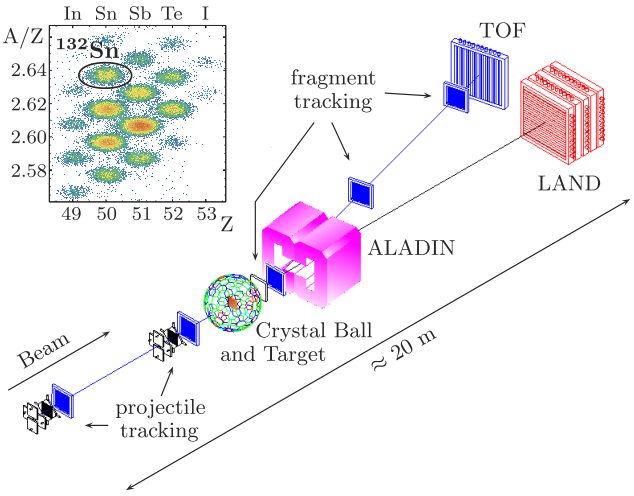

FIG. 1 (color online). Schematic view of the LAND experimental setup. Inset: identification of ^{238}U fission fragments forming the secondary beam.

the isotropically distributed γ background was decreased by 50% while the total calorimetric efficiency, due to the Lorentz boost of the radiation emitted from the heavy fragment, dropped from 70% to 64% only. The γ background was measured independently by selecting events without nuclear reaction, i.e., by requiring no coincident neutrons and no change in mass or charge of the projectile after the target; its mean value of 740 keV (in the forward hemisphere alone) was subtracted from the measured sum of γ radiation energy. The spread of the γ-background distribution ($\sigma = 490$ keV), however, contributes significantly to the detector resolution in excitation energy.

The heavy fragment was identified and momentum analyzed by means of energy-loss and time-of-flight measurements and by tracking in the magnetic field of the dipole magnet ALADIN. Resolutions of $\sigma_Z = 0.2\ e$ for the nuclear charge and of $\sigma_A = 0.45$ u for the nuclear mass were achieved. By combining the information on fragment mass and reconstructed neutron multiplicity, a background of events with wrongly assigned neutron multiplicity could be kept at a level of 20%.

Finally, the excitation energy E^* of the projectiles is obtained from the invariant mass using the measured four-momenta of all decay products, i.e., heavy fragment, neutron(s), and γ rays. Taking into account all instrumental effects, one obtains a non-Gaussian-like detector response, the central part of which exhibits a resolution ranging from $\sigma = 0.7$ to $\sigma = 1.6$ MeV over the relevant range of reconstructed excitation energies.

The electromagnetic cross sections $d\sigma/dE^*$ deduced from the measurement with the Pb target are shown in the left panels of Fig. 2. The data points represent sums of the cross sections in the 1-neutron to 3-neutron decay channels. Background due to reactions occurring outside the target was determined from the measurement without target and was subtracted. The cross section measured with the C target essentially arises from nuclear interactions and was subtracted from that measured with the Pb target after appropriate scaling following the prescription in [16]. The subtracted contribution due to nuclear interactions constitutes about 12% of the cross section measured with the Pb target, both for ^{130}Sn and ^{132}Sn. Efficiency corrections dependent on neutron multiplicity were taken into account. Distortions due to the detector response were not deconvoluted since deconvolution procedures enlarge statistical fluctuations considerably. Instead, parameterized cross sections are convoluted with the detector response function (produced by means of a Monte Carlo simulation) and then compared to the measurement. Both the experimental method and the procedure of data analysis are described in detail in an earlier publication [16] where it was shown that giant resonance cross sections can be reliably extracted in the case of heavy stable isotopes.

In the right-hand panels of Fig. 2, photo-neutron cross sections deduced from the measured Coulomb cross sections are depicted. Here, contributions of the isoscalar and isovector giant quadrupole resonances, calculated with a

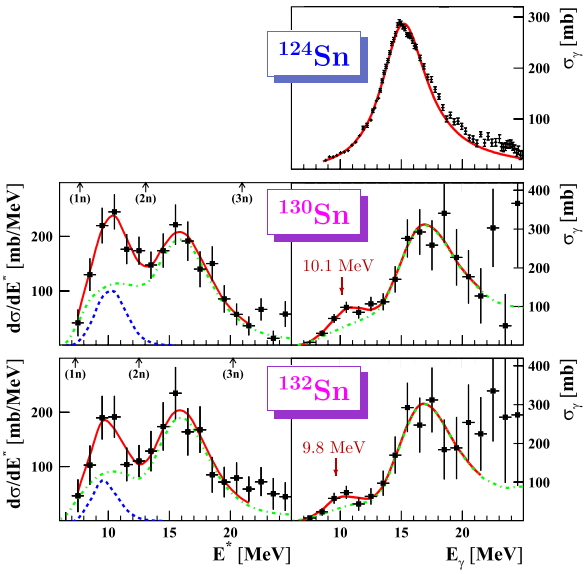

FIG. 2 (color online). Left panels: energy differential, with respect to excitation energy E^*, electromagnetic dissociation cross sections measured in ^{130}Sn and ^{132}Sn. Arrows indicate the neutron-separation thresholds. Corresponding right panels: deduced photo-neutron cross sections. The curves represent fitted Gaussian (blue dashed line) and Lorentzian (green dash-dotted line) distributions, assigned to the PDR (centroid indicated by an arrow) and GDR, respectively, and their sum (red solid line), after folding with the detector response. Top right panel: photo-neutron cross section in the stable ^{124}Sn isotope measured in a real-photon absorption experiment; the solid red line represents a Lorentzian distribution [17].

relativistic Coulomb excitation code and adopting parameters of their strength distribution from data systematics [1], were subtracted from the Coulomb cross sections prior to converting into photo-neutron cross sections. In the top right panel, a photo-neutron spectrum of the heaviest stable tin isotope, ^{124}Sn, measured in a real-photon absorption experiment [17] is shown for comparison. The differences between stable and radioactive tin isotopes at excitation energies around 10 MeV are evident.

In order to extract quantitative information, a Lorentzian distribution of photo-neutron cross section was tentatively adopted to account for the GDR and a Gaussian (or alternatively a Lorentzian) distribution for the apparent low-lying component; below, for convenience, the latter is denoted as PDR. The two distributions are then transformed back to the energy-differential Coulomb cross section, folded with the detector response, and their parameters are found by χ^2 minimization against the experimental data. In this way, positions, widths, and integrated cross sections of both the PDR and GDR peaks are found. The results of this procedure are shown in Fig. 2. The low-energy shoulder of the GDR distribution in part arises because of the rapidly increasing flux of virtual photons towards lower energies, but in part is also of an instrumental nature due to the limited reconstruction efficiency (see above) for the two-neutron decay channel; the latter effect forms about 15% of the cross section observed around the PDR.

A summary of the deduced PDR and GDR parameters is given in Table I; data for the most neutron-rich stable tin isotope, ^{124}Sn, taken from [18] are added for comparison. Deduced parameters for the PDR and GDR peaks are quoted, i.e., peak energy ($E_{\max}$), width (FWHM) and the integral over the photo-neutron cross section ($\int \sigma_\gamma$). The parameters for the PDR did not change significantly if adopting either a Gaussian or a Lorentzian distribution. Because of the finite energy resolution, only an upper limit for the PDR width could be deduced. The errors as quoted in Table I include the correlations among all fitted parameters. As far as the giant dipole resonance parameters are concerned, within error bars no significant deviations from those known for the stable tin isotopes or stable isotopes in the same mass region [1,18] are observed. The essential difference compared to the dipole strength distribution of the stable isotopes is manifested in the appearance of a low-lying component as already noticed. The integrated PDR cross section corresponds to 7(3)% and 4(3)% of the value of the Thomas-Reiche-Kuhn energy-weighted sum rule (EWSR) for ^{130}Sn and ^{132}Sn, respectively. The respective $B(E1)\uparrow$ values amount to 3.2 and 1.9 e^2 fm^2 or to 4.3 and 2.7 Weisskopf units (W.u.), the latter calculated for a neutron transition (for the definition of W.u. adopted here see [1]). Having in mind the well-known strong suppression, compared to the Weisskopf estimate, of $E1$ single-particle transitions, such large $B(E1)$ values indicate that the observed low-lying strength is either composed out of a large number of single-particle transitions in a rather narrow energy interval or involves a coherent superposition of transitions forming a new collective mode.

It should be remembered that the dipole strength is measured only above the one-neutron separation threshold, and thus only part of the low-lying strength may be covered in the present experiment. In fact, recent real-photon measurements on stable $N = 82$ isotones [10] revealed a concentration of $E1$ strength in bound states below the neutron threshold, spread over excitation energies between 5.5 and 8 MeV. The integrated strength exhausts, however, less than 1% of the EWSR. Real-photon scattering experiments to bound states of the stable isotopes ^{116,124}Sn uncovered a concentration of $E1$ strength around 6.5 MeV with $B(E1)$ values, however, of only 0.20 and 0.35 e^2 fm^2, respectively [19]. The QRPA calculations by Tsoneva *et al.* [4], which

TABLE I. Summary of the parameters deduced for the PDR and GDR peaks. The parameters for ^{124}Sn are from [18].

	PDR			GDR		
	$E_{\max}$ [MeV]	FWHM [MeV]	$\int \sigma_\gamma$ [mb MeV]	$E_{\max}$ [MeV]	FWHM [MeV]	$\int \sigma_\gamma$ [mb MeV]
^{124}Sn	...	...	...	15.3	4.8	2080
^{130}Sn	10.1(7)	<3.4	130(55)	15.9(5)	4.8(1.7)	2680(410)
^{132}Sn	9.8(7)	<2.5	75(57)	16.1(7)	4.7(2.1)	2330(590)

are in agreement with the experimental results for ^{124}Sn [19], predict a comparable amount of strength concentrated below the neutron threshold at about 6 MeV excitation energy, also in the heavier tin isotopes $^{126-132}$Sn. Recently, the dipole strength distribution in neutron-rich Sn isotopes was theoretically investigated in relativistic (quasiparticle) random phase approximation (RRPA) [5,6] and in nonrelativistic (quasiparticle) RPA including phonon coupling (RPA-PC) [20]. Common to both types of microscopic calculations is the appearance of low-lying strength in an excitation energy interval of 6–10 MeV, predominantly arising from neutron excitations. In the case of ^{132}Sn, a prominent peak is found at 8.6 MeV in the RRPA and at 9.7 MeV in the RPA-PC calculations. In both calculations, the respective transition densities at the nuclear surface show a vanishing proton contribution and are only built from neutron excitations. In the nuclear interior, the RRPA calculation exhibits protons and neutrons oscillating in phase, the RPA-PC calculation shows different nodes for protons and neutrons. The ratio of the integrated low-lying strength to that of the GDR obtained by the two calculations is compared to our experimental results for ^{130,132}Sn in Table II. Both calculations are essentially in accord with each other and with the data. To some extent, however, the conclusions drawn from the two calculations are in conflict. The RRPA approach identifies transitions, e.g., that at 8.6 MeV in ^{132}Sn, to which quite a number of particle-hole configurations contribute coherently (see Table 3 of [6]) and for which the dynamics typical for a pygmy resonance is claimed, i.e., the vibration of excess neutrons ($N > 50$) at the surface with respect to the core. In contrast, the nonrelativistic approach gives no evidence for transitions involving more than one or two particle-hole configurations.

To judge on the collectivity of the PDR strength one may think of employing so-called dipole cluster sum rules [21,22]. The ''cluster'' sum rules are applicable in the case of less tightly bound valence nucleons which oscillate against the remaining ''core'' nucleons. Strictly speaking, these sum rules are justified only provided an unambiguous decoupling of excitations of valence and core nucleons. If we assume that only neutron excitations contribute to the PDR, the energy-weighted sum rule measures the number N_ν of participating valence neutrons. From our experimental PDR energy-weighted strength for ^{130,132}Sn we would derive on average value around $N_\nu \approx 10$. The non-energy-weighted cluster sum rule measures the fluctuation $\langle R_\nu^2 \rangle$ of the center-of-mass coordinate R_ν of the participating valence neutrons (neglecting the exchange term) [22]. From the measured $B(E1)$ value integrated over the PDR, see above, we would derive a value around $\sqrt{\langle R_\nu^2 \rangle} \approx 0.8$ fm. This small value seems conceivable if we adopt a picture of the participating valence neutrons forming a ''skin'' in the nuclear periphery with not too large spatial correlations among themselves.

In summary, the dipole strength distribution was measured for the first time in unstable neutron-rich tin isotopes, the ^{130}Sn and the doubly magic ^{132}Sn nuclei, for excitation energies from the neutron-separation threshold up to the giant resonance domain. A sizeable strength concentrated at energies well below the GDR region is evident; the observed magnitude of this low-lying strength exceeds considerably that found earlier in bound states near the neutron threshold in stable nuclei. Present-day microscopic calculations agree that the low-lying $E1$ strength arises from oscillations of the excess neutrons but it is under debate to what extent a collective motion is formed.

TABLE II. Ratio of the photo-neutron cross section of the PDR to that of the GDR from this experiment in comparison to the microscopic calculations [5] (RRPA) and [20] (RPA-PC).

	This experiment	RRPA	RPA-PC
^{130}Sn	0.05(2)	0.055	···
^{132}Sn	0.03(2)	0.05	0.04

This work was supported by the German Federal Minister for Education and Research (BMBF) under Contract No. 06MZ174 and by the Polish Committee of Scientific Research under Contract No. 1 P03B 001 27.

[1] M. N. Harakeh and A. van der Woude, *Giant Resonances*, Oxford Studies in Nuclear Physics Vol. 24 (Oxford University, New York, 2001).
[2] Y. Suzuki, K. Ikeda, and H. Sato, Prog. Theor. Phys. **83**, 180 (1990).
[3] P. V. Isacker, M. A. Nagarajan, and D. D. Warner, Phys. Rev. C **45**, R13 (1992).
[4] N. Tsoneva, H. Lenske, and C. Stoyanov, Phys. Lett. B **586**, 213 (2004).
[5] N. Paar, P. Ring, T. Nikšić, and D. Vretenar, Phys. Rev. C **67**, 34312 (2003).
[6] D. Vretenar, N. Paar, P. Ring, and G. A. Lalazissis, Nucl. Phys. **A692**, 496 (2001).
[7] S. Goriely and E. Khan, Nucl. Phys. **A706**, 217 (2002).
[8] A. Leistenschneider *et al.*, Phys. Rev. Lett. **86**, 5442 (2001).
[9] E. Tryggestad *et al.*, Phys. Lett. B **541**, 52 (2002).
[10] A. Zilges *et al.*, Phys. Lett. B **542**, 43 (2002).
[11] N. Ryezayeva *et al.*, Phys. Rev. Lett. **89**, 272502 (2002).
[12] A. Winther and K. Alder, Nucl. Phys. **A319**, 518 (1979).
[13] C. A. Bertulani and G. Baur, Phys. Rep. **163**, 299 (1988).
[14] H. Geissel *et al.*, Nucl. Instrum. Methods Phys. Res., Sect. B **70**, 286 (1992).
[15] T. Blaich *et al.*, Nucl. Instrum. Methods Phys. Res., Sect. A **314**, 136 (1992).
[16] K. Boretzky *et al.*, Phys. Rev. C, **68**, 024317 (2003).
[17] S. C. Fultz *et al.*, Phys. Rev. **186**, 1255 (1969).
[18] S. S. Dietrich and B. L. Berman, At. Data Nucl. Data Tables **38**, 199 (1988).
[19] K. Govaert *et al.*, Phys. Rev. C **57**, 2229 (1998).
[20] D. Sarchi, P. F. Bortignon, and G. Colò, Phys. Lett. B **601**, 27 (2004).
[21] Y. Alhassid and M. Gai, Phys. Rev. Lett. **49**, 1482 (1982).
[22] H. Sagawa and M. Honma, Phys. Lett. B **251**, 17 (1990).